This is a preprint, the final version is subject to change, of the American Mineralogist (MSA)
Cite as Authors (Year) Title. American Mineralogist, in press.
(DOI will not work until issue is live.) DOI: http://dx.doi.org/10.2138/am-2017-6013

Revision 2

Cabvinite, $Th_2F_7(OH)\cdot 3H_2O$, the first natural actinide halide

PAOLO ORLANDI[1], CRISTIAN BIAGIONI[1*], and FEDERICA ZACCARINI[2]

[1] *Dipartimento di Scienze della Terra, Università di Pisa, Via S. Maria 53, I-56126 Pisa, Italy*

[2] *Resource Mineralogy, University of Leoben, Peter Tunner Str. 5, A-8700 Leoben, Austria*

**e-mail address: biagioni@dst.unipi.it*

ABSTRACT

The new mineral species cabvinite, $Th_2F_7(OH)\cdot 3H_2O$ (IMA 2016-011), has been discovered in the Mo-Bi ore deposit of Su Seinargiu, Sarroch, Cagliari, Sardinia, Italy. It occurs as white square prismatic crystals, up to 100 μm in length and 40 μm in thickness, associated with brookite and iron oxy-hydroxides in vugs of quartz veins. Electron microprobe analysis gave (mean of 5 spot analyses, in wt%): ThO_2 82.35, F 19.93, H_2O_{calc} 10.21, sum 112.49, O = -F = -8.40, total 104.09. On the basis of 2 Th atoms per formula unit, the empirical formula of cabvinite is $Th_2F_{6.7}(OH)_{1.3}\cdot 3H_2O$. Main diffraction lines in the X-ray powder diffraction pattern are [*d*(Å) (relative visual intensity) *hkl*]: 8.02 (ms) 110; 3.975 (s) 121, 211; 3.595 (m) (310, 130), 2.832 (m) 400, 321, 231; 2.125 (m) 402; 2.056 (m) 332; and 2.004 (ms) 440, 521, 251. Cabvinite is tetragonal, space group *I*4/*m*, with a = 11.3689(2), c = 6.4175(1) Å, V = 829.47(2) Å^3, Z = 4. The crystal structure has been solved and refined to R_1 = 0.021 on the basis of 813 reflections with $F_o > 4\sigma(F_o)$. It consists of Th tricapped trigonal prisms, connected through corner-sharing, giving rise to a framework hosting [001] tunnels. Cabvinite is the first natural actinide halide, improving the knowledge of the crystal chemistry of actinides and, in particular, of thorium mineralogy.

Key-words: cabvinite, halide, thorium, fluorine, crystal structure, Su Seinargiu, Sardinia, Italy.

INTRODUCTION

Actinide mineralogy is an interesting research field, owing to several applications of Th and U in geoscience and their technological importance, related both to the nuclear power production and to the management of nuclear wastes. Whereas uranium forms more than 250 different mineral species, only few minerals having Th as an essential component have been described (e.g., Hazen et al. 2009). In addition, these species belong to only some classes, i.e. oxides, carbonates, phosphates, and silicates (Table 1). Recently, advance in the knowledge of Th mineralogy has been achieved through the study of the mineral assemblages occurring at the small Mo-Bi prospect of Su Seinargiu, Sarroch, Cagliari, Sardinia, Italy, with the description of the first natural thorium molybdates.

Su Seinargiu, with more than sixty different mineral species so far reported (Orlandi et al. 2015a) and twelve distinct Mo minerals described, can be considered as a reference locality to study Mo mineralogy. Indeed, among these twelve Mo minerals, seven have their type locality at Su Seinargiu, i.e. the Bi-Mo oxides sardignaite, gelosaite, and mambertiite (Orlandi et al. 2010, 2011, 2015b), the REE molybdate tancaite-(Ce) (Bonaccorsi and Orlandi 2010), suseinargiuite, the Na-Bi analogue of wulfenite (Orlandi et al. 2015c), and the two thorium molybdates ichnusaite, $Th(MoO_4)_2 \cdot 3H_2O$, and nuragheite, $Th(MoO_4)_2 \cdot H_2O$ (Orlandi et al. 2014, 2015d). The finding of the first two natural thorium molybdates focused our attention on Th minerals, with the identification of other phases (thorbastnäsite, thorite – Orlandi et al. 2015a) and the first natural thorium halide, cabvinite, herewith described.

This new mineral species (IMA 2016-011) and its name were approved by the IMA-CNMNC. The holotype material of cabvinite is deposited in the mineralogical collections of the Museo di Storia Naturale, University of Pisa, Via Roma 79, Calci, Pisa, Italy, under catalogue number 19711. The name honors two Italian mineral collectors, Fernando Caboni (b. 1941) and Antonello Vinci (b.

1944), for their contribution to the knowledge of the Su Seinargiu mineralogy. Cabvinite is the acronym after their surnames, CABoni and VINci.

OCCURRENCE AND MINERAL DESCRIPTION

Cabvinite was identified on only two small specimens from the Su Seinargiu prospect, Sarroch, Cagliari, Sardinia, Italy. The Mo-Bi mineralization is hosted within Variscan leucogranites (Caboi et al. 1978; Ghezzo et al. 1981) and it is dated to 288.7 ± 0.5 Ma on the basis of the Re-Os age of molybdenite (Boni et al. 2003). Several Mo mineralizations are associated with Variscan leucogranites in Sardinia (Ghezzo et al. 1981) and Su Seinargiu is one of the smallest prospects. Curiously, Caboi et al. (1978) stated that a peculiar feature of the Su Seinargiu Mo-Bi mineralization was related to the small number of different mineral species, with the mineral assemblage formed exclusively by quartz and molybdenite, with trace amounts of chalcopyrite, pyrite, "wolframite", and yellow ochres of Mo. On the contrary, a careful investigation of the Su Seinargiu mineralogy pointed out an outstanding mineral variety, with more than sixty different species, among which are unusual Bi-Mo-Th compounds (e.g., Orlandi et al. 2015a). The majority of these minerals seems to be related to the alteration (probably a low *T* hydrothermal alteration) of the Mo-Bi ores.

Cabvinite occurs as white square prismatic crystals, elongated on [001], up to 100 μm in length and 40 μm in thickness (Fig. 1). It is transparent, with a vitreous luster. Streak is white. Cabvinite is brittle; scanning electron microscope images suggest the occurrence of a {001} cleavage or parting. Owing to the very small amount of available material and its small size, micro-indentation hardness, density, as well as optical properties, were not measured. On the basis of the ideal formula, the calculated density is 5.35 g/cm^3. The mean refractive index of cabvinite, obtained from the Gladstone-Dale relationship (Mandarino 1979, 1981) using the ideal formula and the calculated density, is 1.838.

Cabvinite occurs in small vugs of quartz veins associated with brookite and iron oxy-hydroxides ("limonite").

CHEMICAL DATA AND MICRO-RAMAN SPECTROMETRY

Preliminary chemical analyses of cabvinite performed through energy dispersive spectrometry showed Th and F as the only elements with $Z > 8$. Quantitative data were obtained through wavelength dispersive spectrometry (WDS mode) with a Superprobe JEOL JXA8200 electron microprobe at the "Eugen F. Stumpfl laboratory", Leoben University, Austria, using the following analytical conditions: accelerating voltage 15 kV, beam current 10 nA, nominal beam diameter 1 μm. The peak and backgrounds counting times were 20 and 10 seconds, respectively. The following diffracting crystals were selected: PETH for Th, and TAP for F. Standards (element, emission line) were: thorianite (Th*M*α) and fluorite (F*K*α). The ZAF routine was applied for the correction of recorded raw data. Five spot analyses were performed on a polished grain that was found to be homogeneous. Direct H_2O determination was not performed owing to the scarcity of available material but its occurrence was first suggested by the structural study and then confirmed by micro-Raman spectrometry (see below). Chemical data are given in Table 1; the chemical formula, based on 2 Th atoms per formula unit (apfu), assuming 3 H_2O groups and (OH+F) = 8 apfu, is $Th_2F_{6.7}(OH)_{1.3}\cdot 3H_2O$. The ideal formula of cabvinite is $Th_2F_7(OH)\cdot 3H_2O$, corresponding to (in wt%) ThO_2 79.04, H_2O 9.44, F 19.90, O (≡ F) -8.38, sum 100.00.

Unpolarized micro-Raman spectra were collected on an unpolished sample of cabvinite in nearly back-scattered geometry with a Jobin-Yvon Horiba XploRA Plus apparatus, equipped with a motorized *x*-*y* stage and an Olympus BX41 microscope with a 10× objective. The Raman spectra were excited using a 532 nm line of a solid state laser attenuated to 50%. The minimum lateral and depth resolution was set to a few μm. The system was calibrated using the 520.6 cm^{-1} Raman band of silicon before each experimental session. Spectra were collected through multiple acquisitions with single counting times of 60 s. Backscattered radiation was analyzed with a 1200 mm^{-1} grating

monochromator. Peak deconvolution was performed using the software Fityk (Wojdyr 2010). The Raman spectrum of cabvinite shows few bands, located below 600 cm^{-1}, as usual for several fluorides (e.g., Li_3ThF_7 – Oliveira et al. 1999). Relatively strong bands occur at 113, 209, 342, and 461 cm^{-1} (Fig. 2a) which could be interpreted as lattice vibrations or Th–F modes. A strong and broad band occur in the region between 3000 and 3800 cm^{-1} (Fig. 2b) which could be attributed to the O–H stretching vibrations. The deconvolution of such a band indicated the occurrence of two main bands at 3257 and 3407 cm^{-1}. By using the relationship between O–H stretching frequencies and O···O distances proposed by Libowitzky (1999), these Raman bands could correspond to hydrogen bonds having O···O distances of 2.72 and 2.80 Å, respectively.

X-RAY CRYSTALLOGRAPHY AND STRUCTURE REFINEMENT

X-ray powder diffraction pattern of cabvinite was collected using a 114.6 mm diameter Gandolfi camera and Ni-filtered Cu*K*α radiation. The observed X-ray powder diffraction pattern is given in Table 2. Unit-cell parameters, refined using UnitCell (Holland and Redfern 1997) on the basis of 15 unequivocally indexed reflections, are a = 11.370(1), c = 6.424(1) Å, V = 830.5(1) $Å^3$.

Single-crystal X-ray diffraction data were collected using a Bruker Smart Breeze diffractometer equipped with an air-cooled CCD area detector. Graphite-monochromatized Mo*K*α radiation was used. The detector-to-crystal distance was 50 mm. 1455 frames were collected using ω and φ scan modes, in 0.5° slices, with an exposure time of 25 s per frame. Data were integrated and corrected for Lorentz-polarization, background, and absorption, using the package of software Apex2 (Bruker AXS Inc. 2004). The statistical tests on the distribution of $|E|$ values ($|E^2-1|$ = 0.840) indicated the possible presence of an inversion center. The unit-cell parameters of cabvinite are similar to those of synthetic $Th_2F_7(AuF_4)$ (Schmidt and Müller 1999), i.e. a = 11.306(1), c = 6.313(1) Å, V = 807.0(1) $Å^3$, space group *I*4/*mcm*, to be compared with those observed in cabvinite, i.e. a = 11.3689(2), c = 6.4175(1) Å, V = 829.47(2) $Å^3$. Consequently, the crystal structure of cabvinite was initially refined using Shelxl-2014 (Sheldrick 2015) starting from the atomic

coordinates of the synthetic compound. The site labeled Au in the crystal structure of synthetic $Th_2F_7(AuF_4)$ was found to be completely empty. The refinement converged to $R_1 = 0.052$, giving reasonable Th–φ (φ = F, O) distances. However, a maximum residual of about 5.5 e/Å^3 was unexplained, being located at 1.50 Å from one anion position. In addition, some weak reflections did not match the chosen space group symmetry. Therefore, the crystal structure was solved by direct methods using Shelxs-97 (Sheldrick 2008) in the space group $I4/m$, assuming the occurrence of a {100} twin plane. The crystal structure solution allowed the identification of one Th position and five anion sites. Curves for neutral atoms were taken from the *International Tables for Crystallography* (Wilson 1992). An anisotropic model for all atom positions but one (the only exception being represented by Ow5) achieved a final $R_1 = 0.0209$ on the basis of 813 reflections with $F_o > 4\sigma(F_o)$. Twin ratio is 0.49(1), likely indicating a perfect merohedral twinning. Details of the selected crystal, data collection, and refinement are given in Table 3.

CRYSTAL STRUCTURE DESCRIPTION

Atom coordinates, site occupancies, and displacement parameters are reported in Table 4, whereas selected bond distances and bond-valence sums (BVS, in valence unit, *v.u.*), calculated using the bond parameters of Brese and O'Keeffe (1991), are given in Table 5.

The crystal structure of cabvinite (Fig. 3) has one symmetrically unique cation site and five anion positions. Thorium occurs in a tricapped trigonal prismatic coordination, forming a $ThF_7(OH)_{0.5}(H_2O)_{1.5}$ polyhedron. Th–φ distances range between 2.318 (Th–F1) and 2.585 Å (Th–Ow5), with average bond distance of 2.385 Å. Its BVS is 4.09 v.u., in agreement with the formal charge of Th, i.e. +4. Thorium-centered polyhedra are connected through corner-sharing, giving rise to a framework hosting [001] tunnels. Fluorine is hosted at the F1, F2, and F3 sites, whereas O4 and Ow5 are mixed (OH, H_2O) and pure H_2O sites, respectively. The anion sites F1, F2, and F3 are two-fold coordinated by Th, and have BVS of 1.02, 0.94, and 0.96 v.u., respectively, in agreement with

their occupancy by fluorine anions. Atoms hosted at O4 and Ow5 sites are undersaturated with respect to the bond-valence requirements, with BVS of 0.42 and 0.32 v.u., respectively.

Figure 4 shows an hypothetical hydrogen bond system involving O4 and Ow5 sites. Short O···O distances are represented by O4···O4 and Ow5···Ow5 distances, i.e. 2.66(1) and 2.73(2) Å, respectively, lying in the (001) plane; along **c**, the O4···Ow5 distance is relatively long, i.e. 3.29(1) Å. By using the relationship of Ferraris and Ivaldi (1988), the bond strengths of the O4···O4, Ow5···Ow5, and O4···Ow5 distances are 0.26, 0.22, and 0.09 v.u., respectively. In the model proposed in Figure 4, the O4 site could be occupied by OH^- or H_2O groups. In the first case (i), O4 is acceptor of two hydrogen bonds from two symmetry-related O4 and from an H_2O group hosted at the Ow5 site along +**c**; moreover, the OH^- group is donor in a long O4···Ow5 bond along -**c**. In this configuration, the BVS at the O4 site is 0.94 v.u. In the second case (ii), O4 is donor in two hydrogen bonds with symmetry-related O4 (hosting OH^- groups) and it is acceptor of an hydrogen bond from Ow5; its BVS is -0.01 v.u. Ow5 is acceptor and donor of hydrogen bonds with symmetry-related Ow5 sites within the (001) plane; in addition, it could be acceptor and donor with OH^- groups hosted at O4 belonging to consecutive planes along **c** (iii) or it could be donor with H_2O groups hosted at O4 (iv). In the first case, its BVS is 0.32 v.u., whereas in the second case the BVS is 0.23 v.u. The relatively high BVS at Ow5 site could be a consequence of the inaccuracy of the location of this oxygen atom, in agreement with its relatively high displacement parameter.

The crystal-chemical formula of cabvinite, derived from the crystal structure study, is $Th_2F_7(OH)\cdot 3H_2O$ ($Z = 4$).

DISCUSSION

Cabvinite is the first thorium halide known in nature. It belongs to the 03.D group of the Strunz and Nickel classification, i.e. oxyhalides, hydroxyhalides and related double halides (Strunz and Nickel 2001), being a hydrated thorium hydroxyfluoride. The only other mineral containing Th and F as essential components is the fluorcarbonate thorbastnäsite, described by Pavlenko et al.

(1965) from Eastern Siberia, Russia. Unfortunately, its crystal structure has not been solved yet. On the contrary, several thorium fluorides have been synthesized. Some of them are microporous compounds, with a Th–F framework forming channels hosting alkali metals (e.g., $CsTh_6F_{25}$, $NaTh_3F_{13}$, $CsTh_3F_{13}$, $RbTh_3F_{13}$; Underwood et al. 2011, 2012). Following the IUPAC recommendations (Rouquérol et al. 1994), cabvinite can be described as a microporous compound too. As described above, Schmidt and Müller (1999) obtained synthetic $Th_2F_7(AuF_4)$, that can be derived from cabvinite through the substitution $\square + [(OH)^- + 3H_2O] = Au^{3+} + 4F^-$, with Au^{3+} being host within the channels. The unit-cell volume of cabvinite is larger than that of the synthetic compound, i.e. 829.5 $Å^3$ vs 807.0 $Å^3$, respectively, corresponding to $\Delta V = +2.8\%$. The expansion of the unit-cell volume of cabvinite is in line with the empty nature of the Au site occurring in the [001] tunnels of the synthetic compound. In cabvinite, tunnels host the H atoms of OH^- and H_2O groups. In addition to the thorium synthetic compound, Schmidt and Müller (2004) were able to obtain the U isotype $U_2F_7[AuF_4]$.

Cabvinite is likely the product of the alteration of the primary Mo-Bi ore at Su Seinargiu; the source of thorium is not well-known but other secondary Th minerals like ichnusaite, nuragheite, and thorbastnäsite seem to be related to the same hydrothermal alteration event. Orlandi et al. (2014) observed the presence of corroded crystals of xenotime-(Y) in the same kind of occurrence of ichnusaite, suggesting that the dissolution of xenotime-(Y) could be the source of Th. Finally, the presence of F in the hydrothermal fluids could have favored the solubility and mobility of Th (e.g., Langmuir and Herman 1980; Wood and Ricketts 2000).

IMPLICATIONS

The study of the small Su Seinargiu Mo-Bi mineralization provided the mineral systematics with three very rare Th compounds, i.e. the two thorium molybdates ichnusaite and nuragheite and the thorium fluoride cabvinite. Ichnusaite was cited by Hazen and Ausubel (2016) as an example of rarity in the mineral kingdom. Cabvinite is a further notable example of such a rarity, being the first

thorium halide known on the Earth. Following Hazen and Ausubel (2016), rarity can be due to i) restricted phase stability in *P*-*T*-*X* space, ii) incorporation of rare combinations of elements, iii) degradation under ambient conditions, and iv) negative sampling biases. The *P*-*T*-*X* conditions governing the crystallization of cabvinite are not known. Notwithstanding the well-known role played by F in favouring the Th mobility (e.g., Langmuir and Herman 1980), no thorium fluorides were found so far. Consequently, the crystallizing conditions occurring at Su Seinargiu would have been very unusual; this locality seems to be a natural laboratory for the study of Th mobility, with the late-stage crystallization of Th fluorides, fluorcarbonates, and molybdates. Taking into account the restricted conditions favouring the Th mobilization, a careful study of the fluid-rock interactions occurring at Su Seinargiu is mandatory, in order to achieve a better knowledge of Th geochemistry and its potential dispersion in the environment. In addition to peculiar geochemical conditions required for its crystallization, cabvinite could have been overlooked owing to its appearance similar to that of other common species (e.g., baryte).

Finally, cabvinite represents a new structure type among natural compounds and brings new data to the understanding of actinide mineralogy, thus confirming the central role played by rare minerals to advances in crystal chemistry.

ACKNOWLEDGMENTS

The first specimen of cabvinite was provided by Fernando Caboni. The exceptional mineralogy of Su Seinargiu was unveiled owing to his contribution and to the important efforts of Marzio Mamberti, Giuseppe Tanca, and Antonello Vinci in the sampling of this Sardinian locality. The University Centrum for Applied Geosciences (UCAG) is thanked for the access to the "Eugen F. Stumpfl" electron microprobe laboratory. Marco Pasero is thanked for the critical reading of the manuscript. The constructive comments by Sergey Krivovichev, Jakub Plášil, and an anonymous reviewer helped us in improving the paper.

REFERENCES

Anderson, BW., Claringbull, G.F., Davis, R.J., and Hill, D.K. (1961) Ekanite, a new metamict mineral from Ceylon. Nature, 4780, 997.

Ansell, V.E., and Chao, G.Y. (1987) Thornasite, a new hydrous sodium thorium silicate from Mont St-Hilaire, Quebec. The Canadian Mineralogist, 25, 181-183.

Atencio, D., Carvalho, F.M.S., and Matioli, P.A. (2004) Coutinhoite, a new thorium-uranyl silicate hydrate, from Urucum Mine, Galiléia, Minas Gerais, Brazil. American Mineralogist, 89, 721-724.

Bonaccorsi, E., and Orlandi, P. (2010) Tancaite-(Ce), a new molybdate from Italy. Acta Mineralogica Petrographica Abstract Series. 20th General Meeting of the International Mineralogical Association, 21st–27th August 2010. Budapest, Hungary, 6, 494.

Boni, M., Stein, H.J., Zimmerman, A., and Villa, I.M. (2003) Re-Os age for molybdenite from SW Sardinia (Italy): A comparison with 40Ar/39Ar dating of Variscan granitoids. Mineral Exploration and Sustainable Development, Proceedings of the Seventh Biennial SGA Meeting on Mineral Exploration and Sustainable Development, Athens, Greece, p. 247-250.

Bowie, S.H.U. (1957) Summary of progress of the Geological Survey of Great Britain and the Museum of Practical Geology for the year 1956. Atomic Energy Division, Geological Survey of Great Britain, 1957, 66-67.

Bowie, S.H.U., and Horne, J.E.T. (1953) Cheralite, a new mineral of the monazite group. Mineralogical Magazine, 30, 93-99.

Brese, N.E., and O'Keeffe, M. (1991) Bond-valence parameters for solids. Acta Crystallographica, B47, 192-197.

Bruker AXS Inc. (2004) APEX 2. Bruker Advanced X-ray Solutions, Madison, Wisconsin, USA.

Caboi, R., Massoli-Novelli, R., and Sanna, G. (1978) La mineralizzazione a molibdenite di P.ta de Su Seinargiu (Sarroch – Sardegna meridionale). Rendiconti della Società Italiana di Mineralogia e Petrologia, 34, 167-186.

Cooper, M.A., Abdu, Y.A., Ball, N.A., Černý, P., Hawthorne, F.C., and Kristiansen, R. (2012) Aspedamite, ideally $\square_{12}(Fe^{3+},Fe^{2+})_3Nb_4[Th(Nb,Fe^{3+})_{12}O_{42}]\{(H_2O),(OH)\}_{12}$, a new heteropolyniobate mineral species from the Herrebøkasa Quarry, Aspedammen, Østfold, Southern Norway: description and crystal structure. The Canadian Mineralogist, 50, 793-804.

Della Ventura, G., Bonazzi, P., Oberti, R., and Ottolini, L. (2002) Ciprianiite and mottanaite-(Ce), two new minerals of the hellandite group from Latium (Italy). American Mineralogist, 87, 739-744.

Dunstan, W. (1904) The occurrence of thorium in Ceylon. Nature, 69, 510-511.

Es'kova, E.M., Semenov, E.I., Khomyakov, A.P., Mer'kov, A.N., Lebedeva, S.I., and Dubakina, L.S. (1974) Umbozerite – a new mineral. Doklady Akademii Nauk SSSR, 216, 169-171 (in Russian).

Ferraris, G., and Ivaldi, G. (1988) Bond valence vs bond length in O···O hydrogen bonds. Acta Crystallographica, B44, 341-344.

Gahn, J.G., Berzelius, J., Wallman, C., and Eggertz, H.P. (1817) Examination of some minerals found in the neighbourhood of Fahlun and their situation. Annals of Phylosopky, 9, 452-460.

Ghezzo, C., Guasparri, G., Riccobono, F., Sabatini, G., Pretti, S., and Uras, I. (1981) Le mineralizzazioni a molibdeno associate al magmatismo intrusivo ercinico della Sardegna. Rendiconti della Società Italiana di Mineralogia e Petrologia, 38, 133-145.

Gotman, Y.D., and Khapaev, I.A. (1958) Thorutite – a new mineral of the group of titanites of thorium. Zapiski Vsesoyuznogo Mineralogicheskogo Obshchestva, 87, 201-202 (in Russian).

Hazen, R.M., and Ausubel, J.H. (2016) On the nature and significance of rarity in mineralogy. American Mineralogist, 101, 1245-1251.

Hazen, R.M., Ewing, R.C., and Sverjensky, D.A. (2009) Evolution of uranium and thorium minerals. American Mineralogist, 94, 1293-1311.

Holland, T.J.B., and Redfern, S.A.T. (1997) Unit cell refinement from powder diffraction data: the use of regression diagnostics. Mineralogical Magazine, 61, 65-77.

Kraus, W., and Nolze, G. (1996) PowderCell – a program for the representation and manipulation of crystal structures and calculation of the resulting X-ray powder patterns. Journal of Applied Crystallography, 29, 301-303.

Kupriyanova, I.I., Stolyarova, T.I., and Sidorenko, G.A. (1962) A new thorium silicate – thorosteenstrupine. Zapiski Vserossijskogo Mineralogicheskogo Obshchestva, 91, 325-330 (in Russian).

Langmuir, D., and Herman, J.S. (1980) The mobility of thorium in natural waters at low temperatures. Geochimica et Cosmochimica Acta, 44, 1753-1766.

Libowitzky, E. (1999) Correlation of O–H stretching frequencies and O–H···O hydrogen bond lengths in minerals. Monatshefte für Chemie, 130, 1047-1059.

Mandarino, J.A. (1979) The Gladstone-Dale relationship. Part III. Some general applications. The Canadian Mineralogist, 17, 71-76.

Mandarino, J.A. (1981) The Gladstone-Dale relationship. Part IV. The compatibility concept and its application. The Canadian Mineralogist, 19, 441-450.

Oliveira, M.A.S., Gesland, J.-Y., Pimenta, M.A., and Moreira, R.L. (1999) Raman scattering study of the orthorhombic-to-tetragonal phase transition of a Li_3ThF_7 crystal. Physical Review B, 60, 9983-9989.

Orlandi, P., Pasero, M., and Bigi, S. (2010) Sardignaite, a new mineral, the second known bismuth molybdate: description and crystal structure. Mineralogy and Petrology, 100, 17-22.

Orlandi, P., Demartin, F., Pasero, M., Leverett, P., Williams, P.A., and Hibbs, D.E. (2011) Gelosaite, $BiMo^{6+}_{(2-5x)}Mo^{5+}_{6x}O_7(OH)\cdot H_2O$ ($0 \leq x \leq 0.4$), a new mineral from Su Senargiu

(CA), Sardinia, Italu, and a second occurrence from Kingsgate, New England, Australia. American Mineralogist, 96, 268-273.

Orlandi, P., Biagioni, C., Bindi, L., and Nestola, F. (2014) Ichnusaite, $Th(MoO_4)_2 \cdot 3H_2O$, the first natural thorium molybdate: occurrence, description, and crystal structure. American Mineralogist, 99, 2089-2094.

Orlandi, P., Gelosa, M., Bonacina, E., Caboni, F., Mamberti, M., Tanca, G.A., and Vinci, A. (2015a) Sette nuove specie mineralogiche dalla Sardegna. I minerali della mineralizzazione a molibdeno e bismuto di Su Seinargiu (CA). Rivista Mineralogica Italiana, 39, 84-115.

Orlandi, P., Biagioni, C., Pasero, M., Demartin, F., Campostrini, I., and Merlino, S. (2015b) Mambertiite, $BiMo^{5+}_{2.80}O_8(OH)$, a new mineral from Su Seinargiu, Sardinia, Italy: occurrence, crystal structure, and relationships with gelosaite. European Journal of Mineralogy, 27, 405-415.

Orlandi, P., Biagioni, C., Moëlo, Y., Langlade, J., and Faulques, E. (2015c) Suseinargiuite, $(Na_{0.5}Bi_{0.5})MoO_4$, the Na-Bi analogue of wulfenite, from Su Seinargiu, Sardinia, Italy. European Journal of Mineralogy, 27, 695-699.

Orlandi, P., Biagioni, C., Bindi, L., and Merlino, S. (2015d) Nuragheite, $Th(MoO_4)_2 \cdot H_2O$, the second natural thorium molybdate and its relationships to ichnusaite and synthetic $Th(MoO_4)_2$. American Mineralogist, 100, 267-273.

Pabst, A., and Hutton, C.O. (1951) Huttonite, a new monoclinic thorium silicate with an account of its occurrence, analysis, and properties. American Mineralogist, 36, 60-69.

Pautov, L.A., Agakhanov, A.A., Sokolova, E.V., and Kabalov, Y.K. (1997) Turkestanite, $Th(Ca,Na)_2(K_{1-x}\square_x)Si_8O_{20} \cdot nH_2O$ – a new mineral. Zapiski Vserossijskogo Mineralogicheskogo Obshchestva, 126, 45-55 (in Russian).

Pavlenko, A.S., Orlova, L.P., Akhmanova, M.V., and Tobelko, K.I. (1965) A thorium fluocarbonate, thorbastnaesite. Zapiski Vsesoyuznogo Mineralogicheskogo Obshchestva, 94, 105-113 (in Russian).

Pekov, I.V., Yekimenkova, I.A., and Kononkova, N.N. (1997) Thorosteenstrupine from the Lovozero massif and the isomorphic series steenstrupine – thorosteenstrupine. Zapiski Vserossijskogo Mineralogicheskogo Obshchestva, 126, 35-44 (in Russian).

Perrault, G., and Szymański, J.T. (1982) Steacyite, a new name, and a re-evalution of the nomenclature of "ekanite"-group minerals. The Canadian Mineralogist, 20, 59-63.

Piret, P., and Deliens, M. (1987) Les phosphates d'uranyle et d'aluminium de Kobokobo. IX. L'althupite, $AlTh(UO_2)[(UO_2)_3O(OH)(PO_4)_2]_2(OH)_3 \cdot 15H_2O$, nouveau minéral; propriétés et structure cristalline. Bulletin de Minéralogie, 110, 65-72.

Rouquérol, J., Avnir, D., Fairbridge, C.W., Everett, D.H., Haynes, J.H., Pericone, N., Ramsay, J.D.F., Sings, K.S.W., and Unger, K.K. (1994) Recommendations for the characterization of porous solids. Pure Applied Chemistry, 66, 1739–1758.

Schmidt, R., and Müller, B.G. (1999) $Th_2F_7[AuF_4]$ – dar erste „fluorobasische" Tetrafluoroaurat(III) im system ThF_4/AuF_3. Zeitschrift für anorganische und allgemeine Chemie, 625, 602-604.

Schmidt, R., and Müller, B.G. (2004) Einkristalluntersuchungen an $Cs[AuF_4]$, $Cs[Au_2F_7]$ und $U_2F_7[AuF_4]$. Zeitschrift für anorganische und allgemeine Chemie, 630, 2393-2397.

Sheldrick, G.M. (2008) A short history of SHELX. Acta Crystallographica, A64, 112-122.

Sheldrick, G.M. (2015) Crystal structure refinement with SHELX. Acta Crystallographica, C71, 3-8.

Strunz, H., and Nickel, E.H. (2001) Strunz Mineralogical Tables, 9th edition. E. Schweizerbart Verlag, Stuttgart, 870 p.

348 Underwood, C.C., Mann, M., McMillen, C.D., and Kolis, J.W. (2011) Hydrothermal descriptive
349 chemistry and single crystal structure determination of cesium and rubidium thorium
350 fluoride. Inorganic Chemistry, 50, 11825–11831.
351 Underwood, C.C., McMillen, C.D., and Kolis, J.W. (2012) The crystal structures of $CsTh_6F_{25}$ and
352 $NaTh_3F_{13}$. Journal of Chemical Crystallography, 42, 606–610.
353 van Wambeke, L. (1972) Eylettersite, un noveau phosphate de thorium appartenant à la série de la
354 crandallite. Bulletin de la Société Française de Minéralogie et de Cristallographie, 95, 98-105.
355 Wilson, A.J.C. (1992) International Tables for Crystallography Volume C. Kluwer, Dordrecht.
356 Wojdyr, M. (2010) Fityk: a general-purpose peak fitting program. Journal of Applied
357 Crystallography, 43, 1126-1128.
358 Wood, S.A., and Ricketts, A. (2000) Allanite-(Ce) from the Eocene Casto granite, Idaho: response
359 to hydrothermal alteration. The Canadian Mineralogist, 38, 81-100.
360 Yakovenchuk, V.N., Pakhomovskiy, Y.A., Voloshin, A.V., Bogdanova, A.N., Yamnova, N.A., and
361 Pushcharovskiy, D.Y. (1990) Tuliokite $Na_6BaTh(CO_3)_6 \cdot H_2O$ – a new hydrous carbonate of
362 sodium, barium, and thorium, from alkalic pegmatites of the Khibiny massif (Kola Peninsula).
363 Mineralogiceskij Zhurnal, 12, 74-78 (in Russian).
364

TABLE CAPTIONS

Table 1 – Minerals containing thorium as an essential component. Chemical formulae after the IMA list (updated to September 2016) available at http://nrmima.nrm.se//imalist.htm.

Table 2 – Electron-microprobe data (mean of 5 spot analyses, in wt%) of cabvinite and atoms per formula unit (apfu), on the basis of 2 Th apfu.

Table 3 – Crystal data and summary of parameters describing data collection and refinement for cabvinite.

Table 4 – Site occupancies, atomic coordinates, and isotropic (*) or equivalent isotropic displacement parameters (in $Å^2$) for cabvinite. $U_{eq/iso}$ is defined as one third of the trace of the orthogonalized U_{ij} tensor.

Table 5 – Selected bond distances (in Å) and bond-valence balance (in v.u.) for cabvinite.

FIGURE CAPTIONS

Fig. 1 – Cabvinite, white prismatic crystals, up to 100 μm, with iron oxides in a cavity of a quartz vein (a); SEM image of the crystal used for the crystallographic study (b), showing the prismatic habit and the occurrence of a {001} cleavage or parting. Holotype material. Collection of Museo di Storia Naturale of the Pisa University, catalogue number 19711.

Fig. 2 – Micro-Raman spectrum of cabvinite, in the regions 100-1200 cm^{-1} (a) and 3000-3800 cm^{-1} (b).

Fig. 3 – Crystal structure of cabvinite, as seen down **c**. Symbols: yellow polyhedra = Th site. Circles: green = F sites; red = O4 site; light blue = Ow5 site.

Fig. 4 – Hypothetical hydrogen bond system in cabvinite. Circles: red = O4 site; light blue = Ow5 site. Pink circles represent the hypothetical positions of H atoms.

.

389 **Table 1** – Minerals containing thorium as an essential component. Chemical formulae after the

390 IMA list (updated to September 2016) available at http://nrmima.nrm.se//imalist.htm.

	Chemical formula	Type locality	Ref.
Halides			
Cabvinite	$Th_2F_7(OH)\cdot 3H_2O$	Su Seinargiu, Sardinia, Italy	[1]
Oxides			
Aspedamite	$\square_{12}(Fe^{3+},Fe^{2+})_3Nb_4[(Th(Nb,Fe^{3+})_{12}O_{42}](H_2O,OH)_{12}$	Aspedammen, Østfold, Norway	[2]
Thorianite	ThO_2	Balangoda, Ratnapura, Sri Lanka	[3]
Thorutite	$(Th,U,Ca)Ti_2(O,OH)_6$	Severnyi area, Zardalek alkaline massif, Kyrgyzstan	[4]
Carbonates			
Thorbastnäsite	$ThCa(CO_3)_2F_2\cdot 3H_2O$	Pichikol' alkaline massif, Russia	[5]
Tuliokite	$Na_6BaTh(CO_3)_6\cdot 6H_2O$	Khibiny massif, Kola Peninsula, Russia	[6]
Molybdates			
Ichnusaite	$Th(MoO_4)_2\cdot 3H_2O$	Su Seinargiu, Sardinia, Italy	[7]
Nuragheite	$Th(MoO_4)_2\cdot H_2O$	Su Seinargiu, Sardinia, Italy	[8]
Phosphates			
Althupite	$AlTh(UO_2)_7(PO_4)_4(OH)_5\cdot 15H_2O$	Kobokobo pegmatite, Democratic Republic of Congo	[9]
Cheralite	$CaTh(PO_4)_2$	Kuttakuzhi, Kerala, India	[10]
Eylettersite	$Th_{0.75}Al_3(PO_4)_2(OH)_6$	Kobokobo pegmatite, Democratic Republic of Congo	[11]
Grayite	$(Th,Pb,Ca)PO_4\cdot nH_2O$	Gooddays mine, Mutoko District, Zimbabwe	[12]
Silicates			
Ciprianiite	$Ca_4(Th,REE)_2Al(B_4Si_4O_{22})(OH)_2$	Vetralla, Latium, Italy	[13]
Coutinhoite	$Th_xBa_{1-2x}(UO_2)_2Si_5O_{13}\cdot 3H_2O$	Urucum mine, Minas Gerais, Brazil	[14]
Ekanite	$Ca_2ThSi_8O_{20}$	Ehiliyagoda, Ratnapura, Sri Lanka	[15]
Huttonite	$ThSiO_4$	Gillespie's Beach, New Zealand	[16]
Steacyite	$K_{0.3}(Na,Ca)_2ThSi_8O_{20}$	Mont Saint-Hilaire, Québec, Canada	[17]
Thorite	$ThSiO_4$	Langesundsfjorden, Telemark, Norway	[18]
Thornasite	$Na_{12}Th_3(Si_8O_{19})_4\cdot 18H_2O$	Mont Saint-Hilaire, Québec, Canada	[19]
Thorosteenstrupine	$(Ca,Th,Mn)_3Si_4O_{11}F\cdot 6H_2O$*	Chergilen REE occurrence, Russia	[20]
Turkestanite	$(K,\square)(Ca,Na)_2ThSi_8O_{20}\cdot nH_2O$	Dzhelisu massif, Kyrgyzstan Darai-Pioz Glacier, Tadjikistan	[21]
Umbozerite	$Na_3Sr_4ThSi_8(O,OH)_{24}$	Lovozero massif, Kola Peninsula, Russia	[22]

391 [1] this work; [2] Cooper et al. 2012; [3] Dunstan 1904; [4] Gotman and Khapaev 1958; [5] Pavlenko et al.
392 1965; [6] Yakovenchuk et al. 1990; [7] Orlandi et al. 2014; [8] Orlandi et al. 2015d; [9] Piret and Deliens
393 1987; [10] Bowie and Horne 1953; [11] van Wambeke 1972; [12] Bowie 1957; [13] Della Ventura et al. 2002;
394 [14] Atencio et al. 2004; [15] Anderson et al. 1961; [16] Pabst and Hutton 1951; [17] Perrault and Szymański
395 1982; [18] Gahn et al. 1817; [19] Ansell and Chao 1987; [20] Kupriyanova et al. 1962; [21] Pautov et al.
396 1997; [22] Es'kova et al. 1974.
397 *Note: the chemical formula of thorosteenstrupine could be $Na_{0-5}Ca_{1-3}(Th,REE)_6(Mn,Fe,Al,Ti)_{4-5}(Si_6O_{18})_2[(Si,P)O_4]_6(OH,F,O)_x\cdot nH_2O$ (Pekov et al. 1997).
398
399

400 **Table 2** – Electron-microprobe data (mean of 5 spot analyses, in wt%) of cabvinite and atoms per
401 formula unit (apfu), on the basis of 2 Th apfu.

Oxide	wt%	range	e.s.d.
ThO_2	82.35	81.71 – 83.40	0.67
F	19.93	18.16 – 22.03	1.72
H_2O	10.21	9.08 – 11.18	0.95
Sum	112.49	111.60 – 113.02	0.55
O ≡ - F	-8.40		
Total	104.09		
Element	**apfu**	**range**	**e.s.d.**
Th	2.00	-	-
F	6.73	6.12 – 7.48	0.63
OH	1.27	0.52 – 1.88	0.63
H_2O	3.00	-	-

402

403 **Table 3** – Crystal data and summary of parameters describing data collection and refinement for

404 cabvinite.

Crystal data	
SREF formula	$Th_2F_7(OH)\cdot 3H_2O$
Crystal size (mm)	0.095 x 0.040 x 0.040
Cell setting, space group	Tetragonal, *I*4/*m*
a, *c* (Å)	11.3689(2), 6.4175(1)
V (Å^3)	829.47(2)
Z	4
Data collection and refinement	
Radiation, wavelength (Å)	Mo*K*α, 0.71073
Temperature (K)	293
Detector-to-sample distance (mm)	50
Maximum observed 2θ (°)	71.64
Measured reflections	2605
Unique reflections	825
Reflections $F_o > 4\sigma(F_o)$	813
R_{int} after absorption correction	0.0159
R_σ	0.0167
Range of *h*, *k*, *l*	-16 ≤ *h* ≤ 16 -17 ≤ *k* ≤ 8 -8 ≤ *l* ≤ 9
R_1 [$F_o > 4\ \sigma(F_o)$]	0.0209
R_1 (all data)	0.0213
wR_2 (on F^2_o)	0.0677
Goof	1.041
Number of l.s. parameters	36
Maximum and minimum residual	3.21 (at 0.50 Å from O5) -1.86 (at 0.29 Å from Th)

405
406
407

Table 4 – Site occupancies, atomic coordinates, and isotropic (*) or equivalent isotropic displacement parameters (in Å^2) for cabvinite. $U_{eq/iso}$ is defined as one third of the trace of the orthogonalized U_{ij} tensor.

Site	Wyckoff position	Occupancy	*x*/*a*	*y*/*b*	*z*/*c*	$U_{eq/iso}$
Th	8*h*	$Th_{1.00}$	0.14040(3)	0.35220(3)	0	0.0065(1)
F1	4*c*	$F_{1.00}$	0	½	0	0.020(1)
F2	16*i*	$F_{1.00}$	-0.0015(6)	0.3112(3)	0.2508(6)	0.022(1)
F3	8*f*	$F_{1.00}$	¼	¼	¼	0.034(2)
O4	8*h*	$(OH)_{0.50}(H_2O)_{0.50}$	0.0891(7)	0.1394(8)	0	0.030(2)
Ow5	8*h*	H_2O	0.363(2)	0.400(5)	0	0.064(2)*

Table 5 – Selected bond distances (in Å) and bond-valence balance (in v.u.) for cabvinite.

Th	– F1	2.3177(2)		Th	Σ_{anions}
	– F2	2.326(5) × 2	F1	$^{2\times\rightarrow}0.51$	1.02
	– F3	2.3402(2) × 2	F2	$0.50^{\downarrow\times2}$ $0.44^{\downarrow\times2}$	0.94
	– F2	2.372(5) × 2	F3	$^{2\times\rightarrow}0.48^{\downarrow\times2}$	0.96
	– O4	2.489(9)	O4	0.42	0.94^{i} -0.01^{ii}
	– Ow5	2.585(15)	O5	0.32	0.32^{iii} 0.23^{iv}
			Σ_{cation}	4.09	

Note: left and right superscripts indicate the number of bonds for each anion and cation, respectively. Superscripts i, ii, iii, and iv refer to the possible H-bond schemes involving O4 and Ow5 described in the text.

Fig. 1 – Cabvinite, white prismatic crystals, up to 100 μm, with iron oxides in a cavity of a quartz vein (a); SEM image of the crystal used for the crystallographic study (b), showing the prismatic habit and the occurrence of a {001} cleavage or parting. Holotype material. Collection of Museo di Storia Naturale of the Pisa University, catalogue number 19711.

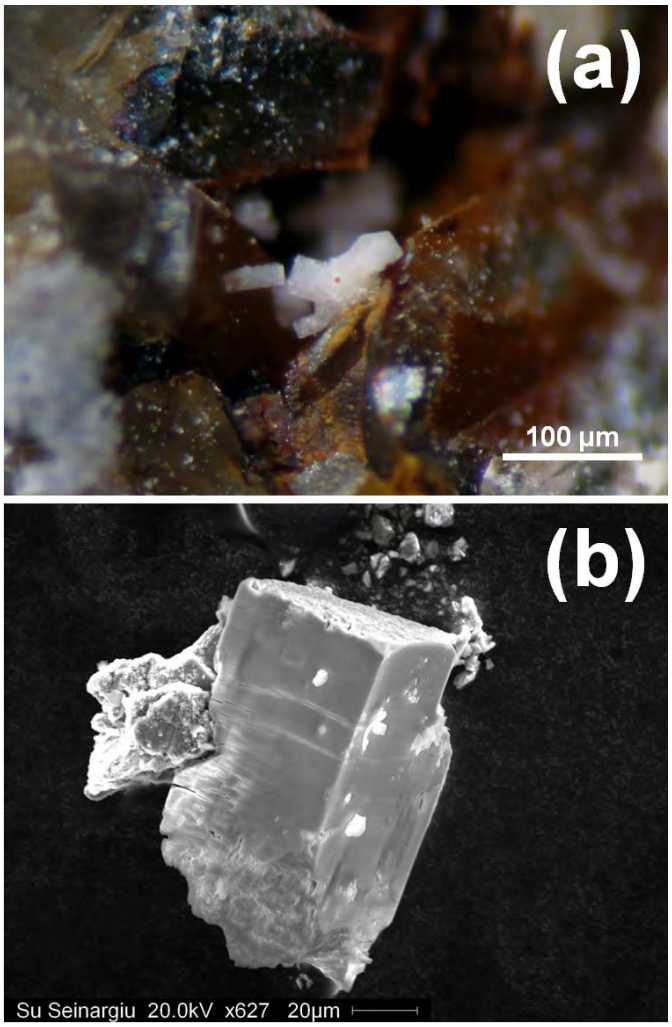

422 **Fig. 2** – Micro-Raman spectrum of cabvinite, in the regions 100-1200 cm^{-1} (a) and 3000-3800 cm^{-1}
423 (b).

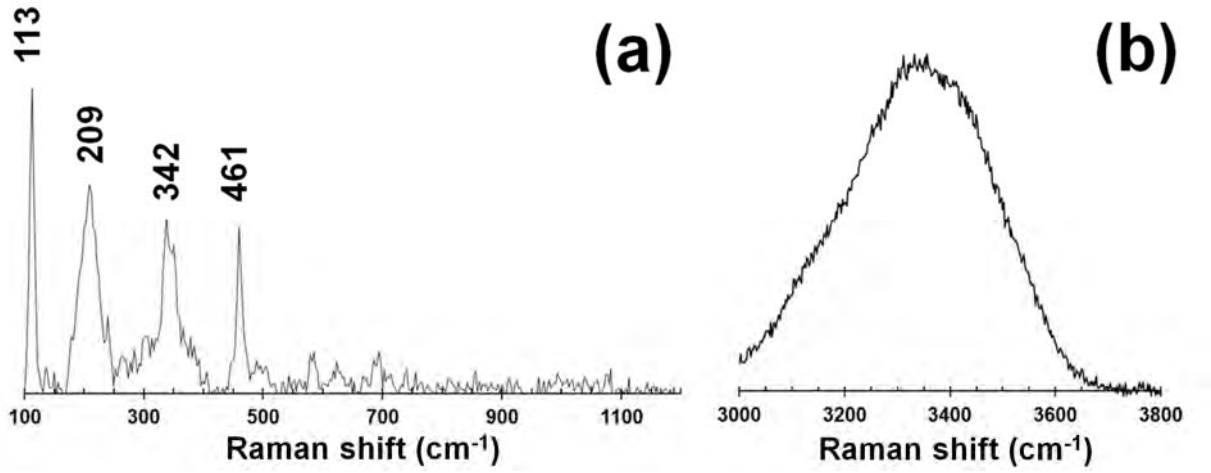

424

425

426 **Fig. 3** – Crystal structure of cabvinite, as seen down **c**. Symbols: yellow polyhedra = Th site.

427 Circles: green = F sites; red = O4 site; light blue = Ow5 site.

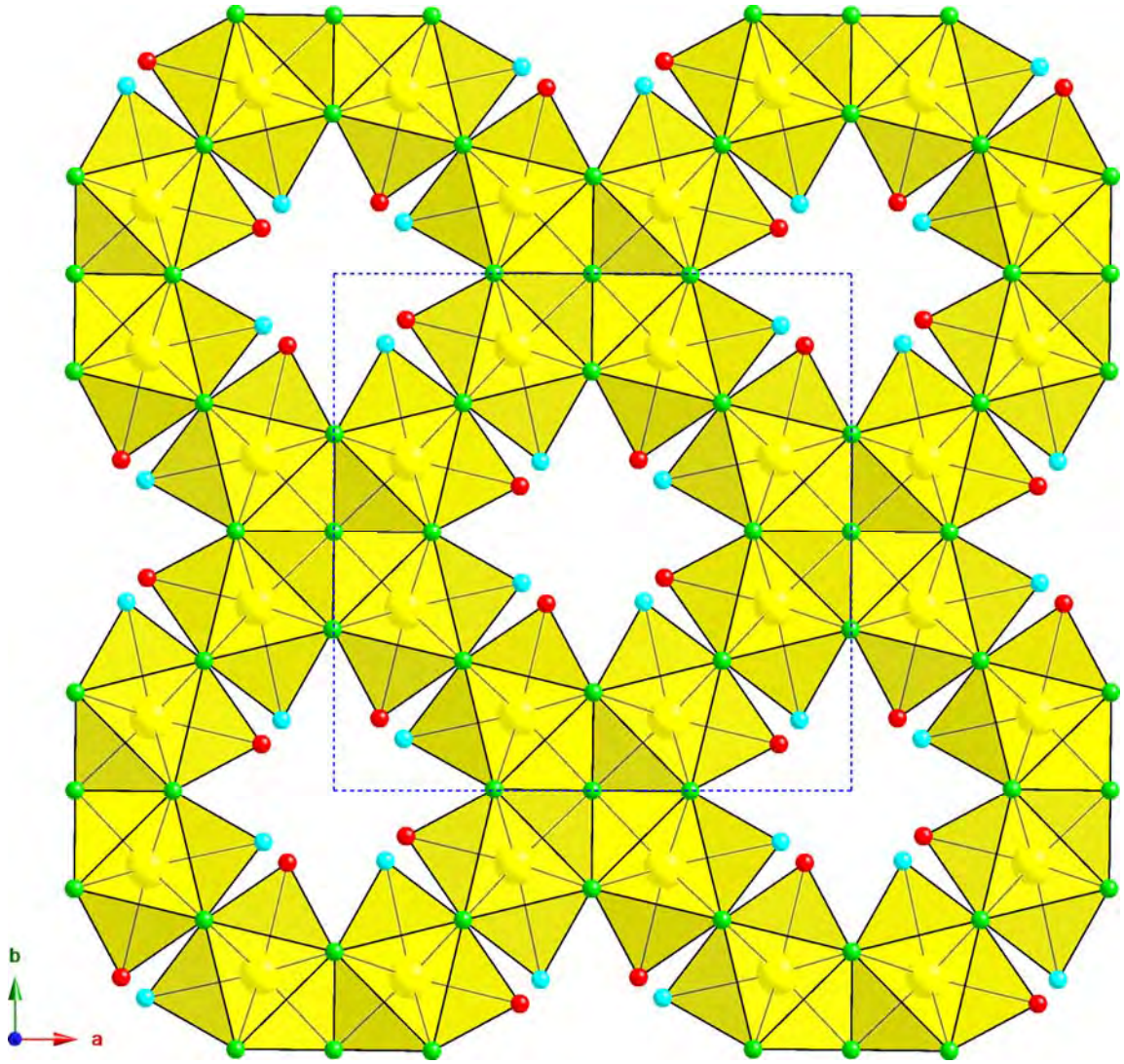

428

429

430

431

Fig. 4 – Hypothetical hydrogen bond system in cabvinite. Circles: red = O4 site; light blue = Ow5 site. Pink circles represent the hypothetical positions of H atoms.